

5.1) We are given Ryden Equation 5.8:

$$\frac{d\varepsilon_i}{\varepsilon_i} = -3(1+w_i)\frac{da}{a} \quad (1)$$

Equation 1 can then be integrated:

$$\int_{\varepsilon_{i,0}}^{\varepsilon_i} \frac{d\varepsilon_i}{\varepsilon_i} = -3(1+w_i) \int_{a_0}^a \frac{da}{a} \quad (2)$$

Assuming that w_i is constant and can be taken out of the rightmost integral. Next,

$$\ln \frac{\varepsilon_i}{\varepsilon_{i,0}} = -3(1+w_i) \ln \frac{a}{a_0} \quad (3)$$

Which can be rearranged:

$$\ln \frac{\varepsilon_i}{\varepsilon_{i,0}} = \ln \left(\frac{a}{a_0} \right)^{-3(1+w_i)} \quad (4)$$

Then, exponentiate and plug in $a_0 = 1$:

$$\boxed{\varepsilon_i(a) = \varepsilon_{i,0} a^{-3(1+w_i)}} \quad (5)$$

Hence, Equation 5 is a valid solution of Equation 1.

As $a \rightarrow 0$, $a^{-3(1+w_i)}$ can approach either infinity or zero. When $-3(1+w_i) > 0$, the energy density approaches zero as the scale factor goes to zero. For $-3(1+w_i) < 0$, the energy density approaches infinity as the scale factor approaches zero. Finally, for $-3(1+w_i) = 0$, the energy density equals $\varepsilon_{i,0}$. We can solve these equations to yield the following:

$$\begin{cases} w_i < -1 \Rightarrow \varepsilon_i \rightarrow 0 \\ w_i > -1 \Rightarrow \varepsilon_i \rightarrow \infty \\ w_i = -1 \Rightarrow \varepsilon_i = \varepsilon_{i,0} \end{cases} \quad (6)$$

From this set of equations, we can see that components with a higher value for w will dominate the energy density for $a \rightarrow 0$. Essentially, any component other than the cosmological constant will have a high energy density, with the higher values of w having higher energy densities. This means that radiation ($w = \frac{1}{3}$) would have had the highest energy density in the early universe.

As $a \rightarrow \infty$, the term, $a^{-3(1+w_i)}$, either approaches infinity or zero. For $-3(1+w_i) > 0$, the energy density approaches infinity, whereas for $-3(1+w_i) < 0$, the energy density approaches zero. We can also have $-3(1+w_i) = 0$, which would yield an energy density that equals $\varepsilon_{i,0}$. Solving these equations gives the following:

$$\begin{cases} w_i < -1 \Rightarrow \varepsilon_i \rightarrow \infty \\ w_i > -1 \Rightarrow \varepsilon_i \rightarrow 0 \\ w_i = -1 \Rightarrow \varepsilon_i = \varepsilon_{i,0} \end{cases} \quad (7)$$

Hence, for $a \rightarrow \infty$, any component with $w_i \leq -1$ will dominate the energy density because the other components' energy density approaches zero.

The cases of $w = 0$ and $w = \frac{1}{3}$ represent the equations for matter and radiation, respectively. For matter ($w = 0$), the equation for energy density would be:

$$\varepsilon_m(a) = \varepsilon_{m,0}a^{-3(1+0)} \quad (8)$$

This can be simplified:

$$\varepsilon_m(a) = \frac{\varepsilon_{m,0}}{a^3} \quad (9)$$

Therefore, the energy density of matter decreases with a^3 . This means that matter would have a high energy density early on in the universe, but that density decreases quite quickly as the universe expands.

We can also solve for the energy density of radiation as a function of a :

$$\varepsilon_r(a) = \varepsilon_{r,0}a^{-3(1+\frac{1}{3})} \quad (10)$$

This can be simplified:

$$\varepsilon_r(a) = \frac{\varepsilon_{r,0}}{a^4} \quad (11)$$

This equation shows that the energy density of radiation decreases with a^4 , which explains why radiation dominates in the early stages of the universe. The energy density of radiation dominates for low values of a and decreases quickly (faster than matter) for higher values.

5.2) From the previous equations, we know that $\varepsilon_\Lambda = \varepsilon_{\Lambda,0}\forall a$ and that $\varepsilon_m(a) = \frac{\varepsilon_{m,0}}{a^3}$. Setting these equal yields

$$\varepsilon_{\Lambda,0} = \frac{\varepsilon_{m,0}}{a^3} \Rightarrow a_{\Lambda m} = \sqrt[3]{\frac{\varepsilon_{m,0}}{\varepsilon_{\Lambda,0}}} \quad (12)$$

Using the definition of the density parameter $\Omega_i = \frac{\varepsilon_i}{\varepsilon_c}$ gives us

$$a_{\Lambda m} = \sqrt[3]{\frac{\Omega_{m,0}}{\Omega_{\Lambda,0}}} = \sqrt[3]{\frac{0.32}{0.68}} \approx 0.778 \quad (13)$$

Using the formula $a = \frac{1}{1+z}$, we have

$$0.778 = \frac{1}{1+z} \Rightarrow z_{\Lambda m} \approx 0.286 \quad (14)$$

Given that in the era of $\Lambda > 0$, the scale factor of the universe increases at an increasing rate, one would expect galaxies to grow at slower speeds for $z \leq 0.286$ because the space between them increases more rapidly during this era. P. Madau & M. Dickinson [3] show with their Figure 9 that the cosmic star formation rate peaks at $z \approx 2$ and then declines for smaller redshifts. This seems to go against what we would expect from the Λ -dominated era, but does not directly contradict the expectation. This is because the cosmological constant is always present, and increases gradually over time; this means that it was active before $z \approx 0.286$. Additionally, the universe was expanding already before Λ -matter equality, so galaxies were already becoming more and more separated. This would naturally allow for a peak in star formation rate at some point. That peak just happens to occur before $z \approx 0.286$.

Galaxy growth and star formation rate are inherently linked, because galaxy mergers can fuel star formation. Ferreira et al. (2020) [2] found an equation that models galaxy merger rates based on redshift for $0.5 \leq z \leq 3$. Their equation is $R(z) = 0.02 \times (1+z)^{2.76}$, not including uncertainties. This equation shows that the galaxy merger rate increases with higher

redshifts, at least up to $z \approx 3$. Beyond merger rates, we can also examine galaxy morphology, as elliptical galaxies tend to be products of the collisions of more complex galaxies, such as spirals. Elmegreen et al. (2005) [1] classified galaxies in the Hubble Ultra Deep Field according to their morphology, and found that 100 of around 900 galaxies were elliptical. This characterizes the galaxies expected for $3 \leq z \leq 7$. On the other hand, Zhao et al. (2018) [4] studied "625 low-redshift brightest cluster galaxies" and described their morphologies. The results of this study showed that 7% of the galaxies were disk-like, compared to a total of 91% for galaxies ranging from cD (central dominant—essentially large ellipticals) to E (elliptical) classifications. These two studies show that more elliptical galaxies exist now than in the past, indicating that past spiral galaxies merged and formed elliptical galaxies.

5.3) Start with the Friedmann equation, generalized for all w :

$$\dot{a}^2 = \frac{8\pi G}{3c^2} \sum_i \varepsilon_{i,0} a^{-1-3w_i} - \frac{\kappa c^2}{R_0^2} \quad (15)$$

We can use Equation 15 to model a single-component universe with $\kappa = 0$:

$$\dot{a}^2 = \frac{8\pi G}{3c^2} \varepsilon_0 a^{-(1+3w)} \quad (16)$$

We can then assume that $a \propto t^q$ (meaning $a = Ct^q$, where C is a constant) so $\dot{a} = Cqt^{q-1}$ and $\dot{a}^2 = C^2 q^2 t^{2q-2}$ so $\dot{a}^2 \propto t^{2q-2}$. Plugging this into Equation 16 gives us

$$t^{2q-2} \propto (t^q)^{-(1+3w)} \Rightarrow t^{2q-2} \propto t^{-q(1+3w)} \quad (17)$$

From this, we have

$$2q - 2 = -q(1 + 3w) \Rightarrow 2q + q(1 + 3w) = 2 \Rightarrow q(2 + 1 + 3w) = 2 \Rightarrow \boxed{q = \frac{2}{3 + 3w}} \quad (18)$$

Note that $w \neq -1$. We can then plug Equation 18 into the assumption $a \propto t^q$:

$$a \propto t^{\frac{2}{3+3w}} \quad (19)$$

To change this statement of proportionality into an equation, we must use the fact that $a(t_0) = 1$, meaning that there has to be a constant $t_0^{-\frac{2}{3+3w}}$ to normalize the equation:

$$a(t) = \left(\frac{1}{t_0}\right)^{\frac{2}{3+3w}} t^{\frac{2}{3+3w}} \Rightarrow \boxed{a(t) = \left(\frac{t}{t_0}\right)^{\frac{2}{3+3w}}} \quad (20)$$

We can then differentiate Equation 20:

$$\frac{d}{dt}a = \dot{a} = \frac{d}{dt} \left(\frac{t}{t_0}\right)^{\frac{2}{3+3w}} = \left(\frac{2}{3+3w}\right) \left(\frac{t}{t_0}\right)^{\frac{2}{3+3w}-1} \left(\frac{1}{t_0}\right) \quad (21)$$

Dividing Equation 21 by Equation 20 and using $t = t_0$ gives us

$$H_0 \equiv \left(\frac{\dot{a}}{a}\right)_{t=t_0} = \left(\frac{2}{3+3w}\right) \left(\frac{t_0}{t_0}\right)^{\frac{2}{3+3w}-1} \left(\frac{1}{t_0}\right) \left(\frac{t_0}{t_0}\right)^{\frac{2}{3+3w}} \Rightarrow \boxed{H_0 = \frac{2}{3(1+w)} t_0^{-1}} \quad (22)$$

Then we can solve for t_0 :

$$H_0 = \left(\frac{2}{3+3w}\right) t_0^{-1} \Rightarrow \boxed{t_0 = \frac{2}{3(1+w)} H_0^{-1}} \quad (23)$$

From Equation 18, we have $q = \frac{2}{3}$ for matter ($w = 0$) and $q = \frac{1}{2}$ for radiation ($w = \frac{1}{3}$). This means that in a matter-dominated universe, the scale factor goes with $t^{\frac{2}{3}}$. For a radiation-dominated universe, the scale factor goes with $t^{\frac{1}{2}}$. The time derivatives of these expressions are $\dot{a} \propto \frac{2}{3}t^{-\frac{1}{3}}$ and $\dot{a} \propto \frac{1}{2}t^{-\frac{1}{2}}$, respectively. The latter is greater than the former for $t < 0.180$. Comparing this to Equation 20 shows that a radiation-dominated universe expands faster than a matter-dominated universe for $t < 0.180t_0$.

From Equation 20, we have the following equations depending on the value of w :

$$a(t) = \begin{cases} \left(\frac{t}{t_0}\right)^{\frac{2}{3}} & (w = 0) \\ \left(\frac{t}{t_0}\right)^{\frac{1}{2}} & (w = \frac{1}{3}) \end{cases} \quad (24)$$

From Equation 24, we can draw the same conclusions as above, with the radiation-dominated universe expanding at a faster rate than the matter-dominated universe initially, then the matter-dominated universe expanding faster for $t > 0.180t_0$. Both universes have a derivative that approaches 0 as $t \rightarrow \infty$, meaning that the speed of expansion will decrease over time for both universes, but neither universe will collapse.

From Equation 22, we have the following equations for the Hubble Constant depending on the value of w :

$$H_0 = \begin{cases} \frac{2}{3}t_0^{-1} & (w = 0) \\ \frac{1}{2}t_0^{-1} & (w = \frac{1}{3}) \end{cases} \quad (25)$$

From Equation 25, we can see that the Hubble Constant and age of the universe are related in a different way based on whether the universe is radiation-dominated or matter-dominated. Whereas in our universe the Hubble Time derived from the Hubble Constant is close to the actual age of the universe, these single-component universes have Hubble Constants that are fractions (2/3 and 1/2 for matter and radiation, respectively) of the inverse of the age of the universe.

Equation 23 gives us an expression slightly different than that of Equation 22, although it is a bit more intuitively useful. Plugging in the values of w that correspond to matter- and radiation-dominated universes gives us the following:

$$t_0 = \begin{cases} \frac{2}{3}H_0^{-1} & (w = 0) \\ \frac{1}{2}H_0^{-1} & (w = \frac{1}{3}) \end{cases} \quad (26)$$

Given that the Hubble Time is equal to H_0^{-1} , Equation 26 tells us that the actual age of the universe is 2/3 or 1/2 of the Hubble Time, depending on whether the universe is dominated by matter or radiation, respectively.

5.4) We are given Ryden Equation 5.47:

$$1 + z = \left(\frac{t_0}{t_e}\right)^{2/(3+3w)} \quad (27)$$

Raising each side to the power of $(3 + 3w)/2$ yields

$$(1 + z)^{(3+3w)/2} = \frac{t_0}{t_e} \quad (28)$$

Solving for t_e gives us

$$t_e = \frac{t_0}{(1+z)^{3(1+w)/2}} \quad (29)$$

Next, we can use Equation 23 to replace t_0 with something in terms of w and H_0 :

$$t_e = \left(\frac{2H_0^{-1}}{3(1+w)} \right) \left(\frac{1}{(1+z)^{3(1+w)/2}} \right) \Rightarrow \boxed{t_e(z) = \left(\frac{2}{3(1+w)H_0} \right) \left(\frac{1}{(1+z)^{3(1+w)/2}} \right)} \quad (30)$$

From Ryden Equation 5.33, we know that

$$d_p(t_0) = c \int_{t_e}^{t_0} \frac{dt}{a(t)} \quad (31)$$

into which we can plug in Equation 20:

$$d_p(t_0) = c \int_{t_e}^{t_0} \left(\frac{t_0}{t} \right)^{2/(3+3w)} dt = ct_0^{2/(3+3w)} \int_{t_e}^{t_0} t^{-2/(3+3w)} dt \quad (32)$$

Solving the above integral gives us

$$d_p(t_0) = \frac{ct_0^{2/(3+3w)}}{1 - 2/(3+3w)} \left[t^{1-\frac{2}{3+3w}} \right]_{t_e}^{t_0} = \frac{ct_0^{2/(3+3w)}}{\frac{1+3w}{3+3w}} \left[t_0^{\frac{1+3w}{3+3w}} - t_e^{\frac{1+3w}{3+3w}} \right] \quad (33)$$

Next, distribute:

$$d_p(t_0) = ct_0^{\frac{2}{3+3w} + \frac{1+3w}{3+3w}} \frac{3+3w}{1+3w} - ct_0^{\frac{2}{3+3w}} t_e^{\frac{1+3w}{3+3w}} \frac{3+3w}{1+3w} \quad (34)$$

Then, simplify the exponent of t_0 and factor:

$$d_p(t_0) = ct_0 \frac{3+3w}{1+3w} \left[1 - t_0^{\frac{2}{3+3w} - \frac{3+3w}{3+3w}} t_e^{\frac{1+3w}{3+3w}} \right] = ct_0 \frac{3+3w}{1+3w} \left[1 - t_0^{\frac{-1-3w}{3+3w}} t_e^{\frac{1+3w}{3+3w}} \right] \quad (35)$$

We can further simplify:

$$\boxed{d_p(t_0) = ct_0 \frac{3(1+w)}{1+3w} \left[1 - \left(\frac{t_e}{t_0} \right)^{\frac{1+3w}{3+3w}} \right]} \quad (36)$$

We can then use Equation 23 and Equation 29 to make Equation 36 in terms of H_0 and z :

$$d_p(t_0) = c \frac{2}{3(1+w)} H_0^{-1} \frac{3(1+w)}{1+3w} \left[1 - \left(\frac{t_0}{(1+z)^{3(1+w)/2}} \frac{1}{t_0} \right)^{\frac{1+3w}{3+3w}} \right] \quad (37)$$

We can then simplify Equation 37 significantly:

$$d_p(t_0) = \frac{c}{H_0} \frac{2}{1+3w} \left[1 - (1+z)^{\frac{1+3w}{3+3w} \cdot \frac{-(3+3w)}{2}} \right] \quad (38)$$

Further simplification yields the following:

$$\boxed{d_p(t_0) = \frac{c}{H_0} \frac{2}{1+3w} \left[1 - (1+z)^{\frac{-(1+3w)}{2}} \right]} \quad (39)$$

Figure 1 shows the graphs of $d_p(t_0)$ and $t_e(z)$ for $w = 0$ (red) and for $w = \frac{1}{3}$ (blue). The Figure 1 graphs use the following formulae for matter ($w = 0$) only:

$$d_{p,m}(t_0) = \frac{c}{H_0} \cdot 2 \left[1 - (1+z)^{-\frac{1}{2}} \right] \quad (40)$$

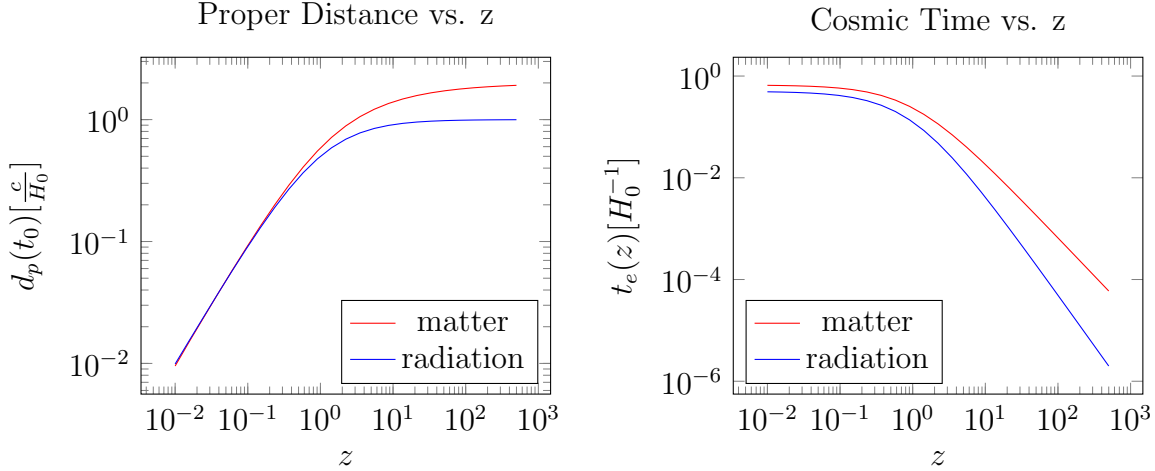


FIGURE 1. Proper distance and cosmic time for radiation- and matter-dominated universes as a function of redshift

$$t_{e,m}(z) = \frac{1}{H_0} \cdot \frac{2}{3} \left(\frac{1}{(1+z)^{3/2}} \right) \quad (41)$$

For radiation only ($w = \frac{1}{3}$), the following formulae are used:

$$d_{p,r}(t_0) = \frac{c}{H_0} \cdot [1 - (1+z)^{-1}] \quad (42)$$

$$t_{e,r}(z) = \frac{1}{H_0} \cdot \frac{1}{2} \left(\frac{1}{(1+z)^2} \right) \quad (43)$$

The graphs are plotted using Equations 40-43, but normalized to eliminate the influence of the Hubble Constant and speed of light. The proper distance is in units of $\frac{c}{H_0}$ (the Hubble Length) and the cosmic time is in units of H_0^{-1} (the Hubble Time).

The graph of proper distance and redshift shows that proper distance changes much faster at low redshifts for a matter-only universe, and then reaches an asymptote for high redshifts. This is because of the faster expansion of the universe in the beginning, so redshift increases more rapidly as one goes back closer to the big bang. The fact that proper distance increases more rapidly for low redshifts is a reflection of the universe not expanding as much over time. Essentially, this graph shows that proper distance increases rapidly as redshift increases a little, then as redshift gets higher, proper distance starts increasing at a slower rate.

The graph of time emitted and redshift for the matter-only universe shows that for low redshifts, the time emitted has a smaller magnitude of its slope, while at higher redshifts, time emitted has a steeper slope (downward). This reflects how at low redshifts, the universe has not expanded as much, so the time that observed light was emitted is not decreasing at a fast rate. For higher redshifts, however, the expansion of the universe plays a bigger role so the slope is steeper.

The graphs for a radiation-dominated universe are very similar to that of a matter-dominated universe. However, the equations are different, causing the proper distance for the radiation-dominated universe to not reach as large of a distance compared to the matter-dominated universe. For the plot of time emitted, the slope of the graph for the radiation-dominated universe is on the order of -2, compared to $-3/2$ for the matter-dominated universe.

REFERENCES

- [1] Debra Meloy Elmegreen et al. “Galaxy Morphologies in the Hubble Ultra Deep Field: Dominance of Linear Structures at the Detection Limit”. In: *The Astrophysical Journal* 631.1 (Sept. 2005), pp. 85–100. ISSN: 1538-4357. DOI: 10.1086/432502. URL: <http://dx.doi.org/10.1086/432502>.
- [2] Leonardo Ferreira et al. “Galaxy Merger Rates up to $z = 3$ Using a Bayesian Deep Learning Model: A Major-merger Classifier Using IllustrisTNG Simulation Data”. In: *The Astrophysical Journal* 895.2 (June 2020), p. 115. ISSN: 1538-4357. DOI: 10.3847/1538-4357/ab8f9b. URL: <http://dx.doi.org/10.3847/1538-4357/ab8f9b>.
- [3] Piero Madau and Mark Dickinson. “Cosmic Star-Formation History”. In: *Annual Review of Astronomy and Astrophysics* 52.1 (Aug. 2014), pp. 415–486. ISSN: 1545-4282. DOI: 10.1146/annurev-astro-081811-125615. URL: <http://dx.doi.org/10.1146/annurev-astro-081811-125615>.
- [4] Dongyao Zhao, Alfonso Aragón-Salamanca, and Christopher J. Conselice. “The link between morphology and structure of brightest cluster galaxies: automatic identification of cDs”. In: *Monthly Notices of the Royal Astronomical Society* 448.3 (Mar. 2015), pp. 2530–2545. ISSN: 0035-8711. DOI: 10.1093/mnras/stv190. URL: <http://dx.doi.org/10.1093/mnras/stv190>.